An Experimental Study on Bond Strength of Reinforcing Steel in High-Volume Fly-Ash Concrete

Jonathan T. Drury[1], Trevor J. Looney[1], Mahdi Arezoumandi[2], Jeffery S. Volz[1]

[1]University of Oklahoma, Civil Engineering and Environmental Science, 202 W. Boyd St., Room 334, Norman, OK 73019-1024
[2]Missouri University of Science & Technology, Dept. of Civil, Architectural, and Environmental Engineering, 1401 N. Pine St., Room 219, Rolla, MO 65409

KEYWORDS: high-volume fly-ash concrete, conventional concrete, bond strength, experimental study

ABSTRACT

The production of Portland cement—the key ingredient in concrete—generates a significant amount of carbon dioxide. However, because of its incredible versatility, availability, and relatively low cost, concrete is the most consumed manmade material on the planet. One method of reducing concrete's contribution to greenhouse gas emissions is the use of fly ash to replace a significant amount of the cement. An experimental investigation was conducted to compare the bond strength of reinforcing steel in high-volume fly-ash concrete (HVFAC)—concrete with at least 50 % of the cement replaced with fly ash—with conventional concrete (CC). This study investigated two HVFAC mixes [with one mix having a relatively high total cementitious content (502 kg/m3) and the other mix having a relatively low total cementitious content (337 kg/m3)], as well as a CC mix. Both HVFAC mixes utilized a 70 % replacement of Portland cement with a Class C fly ash. This experimental program consisted of nine full-scale beams (three for each concrete type). The pull-out specimens were based on RILEM recommendations, and the beam specimens were tested under a simply supported four-point loading condition. The CC test results served as a control and were used to evaluate the results from the HVFAC pull-out and beam specimen tests. Furthermore, a comparison was performed between results of this study and a bond database of CC specimens. These comparisons indicate that HVFAC beams possess greater bond strength than CC beams.

INTRODUCTION

Concrete is the most widely used manmade material in the world, and cement is an essential ingredient in the production of Portland cement concrete. The cement industry plays a key role in the world, from both an economic and an environmental perspective. In 2011, world cement output was estimated at 3.4 x 10^9 metric tons [1]. Cement

production is also a relatively significant source of global carbon dioxide (CO2) emissions, accounting for approximately 4.5 % of global CO2 emissions from industry in 2007 [2]. According to the World Business Council for Sustainable Development (WBCSD), the manufacture of cement emissions varies across worldwide regions from 0.73 to 0.99 kg of CO2 for each kilogram of cement produced [3].

One of the solutions for this global concern is the use of supplementary cementitious materials as a replacement of cement. The most available supplementary cementitious material worldwide is fly ash, a by-product of coal-burning thermal power stations [4]. ASTM C618 [5] defines fly ash as “the finely divided residue that results from the combustion of ground or powdered coal and that is transported by flue gasses.” Fly ash is categorized in three classes: N, F, and C, based on chemical composition [6].

Fly ash has been used in the U.S. since 1930; Davis et al. (1937) were the first researchers to publish their results about using fly ash in concrete [6]. Initially, fly ash was used in massive structures like the Thames Barrage in the U.K. and the Upper Stillwater Dam in the U.S., with about 30 % to 75 % mass replacement of hydraulic cement to reduce heat generation [6]. Subsequent research [7–11] has shown some beneficial aspects of using fly ash in concrete, such as low permeability and high durability.

Traditionally, fly ash used in structural concrete as a replacement or supplementary material is limited to 15 % to 25 % cement replacement [12,13] except in high-strength concrete (HSC), where replacement levels of Portland cement at 35 % are more common to control peak hydration temperature development [14]. When a significant amount of fly ash is used, how it contributes to the strength development of the concrete and the hydration characteristics of this type of material are of significant research interest. High-volume fly-ash concrete (HVFAC) is a concrete generally defined with at least 50 % of the Portland cement replaced with fly ash. In 1986, the Canadian Centre for Mineral and Energy Technology (CANMET) developed HVFAC for structural applications. The investigations by CANMET [15] and other researchers [16,17] have shown that HVFAC has lower shrinkage, creep, and water permeability and higher modulus of elasticity compared with conventional concrete (CC).

Comprehensive research has been done on both the fresh and hardened properties of HVFAC, but very little research has been performed on the structural behavior of HVFAC. Naik et al. [18] performed pull-out tests on specimens with fly-ash replacements of 10 %, 20 %, and 30 % of Port-land cement. The researchers concluded that the bond strength improved with the increase in fly ash up to about 20 % cement replacement, and, after that, it began to decrease. Researchers at Montana State University [19] performed a series of pull-out tests on specimens utilizing 100 %Class C fly ash as a replacement of Portland cement. The specimen design involved #13 bars embedded into a concrete cylinder (150 x 300 mm2). The embedment depth was varied from 200 to 300 mm for each material. Results of this study indicated lower bond strength for HVFAC com-pared to normal concrete. Gopalakrishnan [20] conducted pullout tests to determine the effects of using 50 % fly-ash replacement of cement on

bond strength. Specimens had #20 bars embedded into a 150-mm concrete cube. The researchers reported identical bond strength for HVFAC and CC specimens.
The following study presents the results of an experimental investigation that compares the bond strength of nine full-scale HVFAC and CC beams. The results of this study were also compared with a bond database of CC beam specimens.

EXPERIMENTAL PROGRAM

Several different methods are used to study the bond between steel reinforcement and concrete. The four most common methods are pull-out specimens, beam-end specimens, beam anchorage specimens, and beam splice specimens. The last three methods provide more realistic measures of bond strength compared with pull-out specimen tests [21]. However, the pull-out specimen is more popular because of ease of construction and simplicity of the test. The main drawback with this test is that the stress state does not reflect the actual stress state within a reinforced concrete member. In the pull-out specimen test, the bar is in tension and the concrete surrounding the bar is in compression, but in most reinforced concrete members, both the bar and the surrounding concrete are in tension. For this reason, ACI 408 does not recommend the pull-out specimen test to determine development length of reinforcement. The current study used beam splice specimens to evaluate HVFAC reinforcement bond strength compared with CC.

SPECIMEN DESIGN

Nine beams (three for each concrete type) were designed to preclude flexural and shear failures and satisfy the minimum and maximum longitudinal reinforcement requirements of ACI 318-08 [22]. The beams measured 3000 mm in length, with a cross section of 300 □ 460 mm2, and a splice in the longitudinal steel centered at midspan. The longitudinal steel consisted of three #19 bars, whereas the shear reinforcement consisted of #10, U-shaped stirrups. One beam of each type was cast upside down to evaluate the top bar effect. The test setup used a simply supported four-point loading condition to place the splice under a uniform stress, as shown in Fig. 1, with the stirrups discontinued within the center portion of the beam to provide an unconfined splice condition. To ensure a bond failure prior to a flexural failure, the splice length was chosen as 70 % of the development length calculated in accordance with Eq 12-1 in ACI 318-08 [22], repeated as Eq 1 here:

$$l_d = \frac{3}{40}\frac{f_y}{\sqrt{f'_c}}\frac{\psi_t\psi_e\psi_s}{(c_b + k_{tr})}d_b$$

where:

l_d= the development length,
f_y= the specified yield strength of reinforcement,
f'_c= the specified compressive strength of concrete,
ψ_t= the reinforcement location modification factor,
ψ_e= the reinforcement coating modification factor,
ψ_s= the reinforcement size modification factor,

c_b= the smaller of the distance from the center of a bar to the nearest concrete surface of one-half the center-to-center spacing of bars being developed,

k_{tr}= the transverse reinforcement index, and

d_b= the nominal diameter of the reinforcing bar.

Based on these calculations, the splice length was 360 mm.

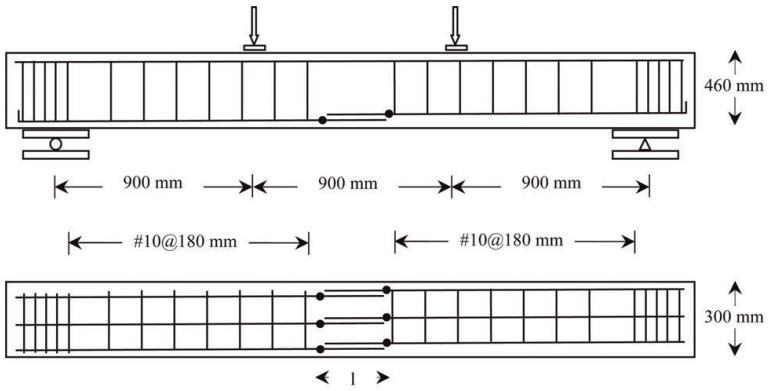

●: Strain gage

a) Beam splice specimen reinforcing layout

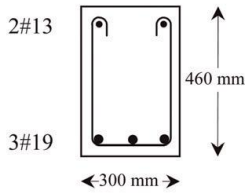

b) Beam splice specimen cross section

c) Splice test setup with specimen loaded

FIG. 1 – Load pattern, cross section, and location of strain gauges on beam.

MATERIALS

The cementitious materials used for this study were ASTM Type I Portland cement; ASTM Class C fly ash from the Ameren Labadie Power Plant (Labadie, MO); gypsum from USA Gypsum (Reinholds, PA); and calcium hydroxide from the Mississippi Lime company (Sainte Genevieve, MO). Table 1 shows the physical properties and chemical compositions of the cement and fly ash.

TABLE 1 – Physical properties and chemical compositions of cement and fly ash.

Physical Properties		
Property	Type-I Cement	Class C Fly Ash
Fineness		
Blaine, m3/kg	347	Not measured
+325 mesh (+44μm)	4.1%	14.4%
Specific gravity	3.15	2.73
Chemical Composition		
Component	Type-I Cement (%)	Class C Fly Ash (%)
SiO_2	21.98	33.46
AL_2O_3	4.35	19.53
Fe_2O_3	3.42	6.28
CaO	63.97	26.28
MgO	1.87	5.54
SO_3	2.73	2.4
Na_2O	0.52 equivalent	1.43 equivalent
LOI	0.60	0.34

The coarse aggregate consisted of crushed limestone with a maximum nominal aggregate size of 19mm from Jefferson City Dolomite (Jefferson City, MO). The fine aggregate was natural sand from Missouri River Sand (Jefferson City, MO).

All of the reinforcing bars were from the same heat of steel, used the same deformation pattern, and met the requirements of ASTM A615 [23], Grade 60, 414-MPa material. Table 2 contains the tested mechanical properties of the reinforcing steel. The rib height, rib spacing, and relative rib area for each bar size was in accordance with ACI 408R [21] and ASTM A615, with the #13 and #19 reinforcing bars used in the pull-out and splice specimens having relative rib areas of 0.088 and 0.081, respectively.

TABLE 2- Mechanical properties of reinforcing steel.

Bar Number	Modulus of Elasticity, MPa	Yielding Strength, MPa	Elongation, mm,mm
13	196,600	485	0.0092
19	206,250	580	0.0085

MIXTURE PROPORTIONS

The concrete mixtures with a target compressive strength of 28 MPa were delivered by a ready-mix concrete supplier (Rolla, MO). The mixture proportions are given in Table 3. The HVFAC mixes used a 70 % replacement of cement with fly ash—with one mix containing a relatively high total cementitious content (502 kg/m3) and the other mix containing a relatively low total cementitious content (337 kg/m3). The designations HVFA-H and HVFA-L represent the relatively high and relatively low total cementitious content HVFAC mixes, respectively. For the HVFAC, the gypsum was used to maintain the initial hydration stage by preventing sulfate depletion, whereas the calcium hydroxide ensured a more complete hydration of the fly ash with the low content of Portland cement in the mix [24]. The drums were charged at the ready-mix facility with the required amounts of cement, fly ash, sand, coarse aggregate, and water, whereas the powder activators (gypsum and lime) were added when the truck arrived at the lab, approximately 5 min later. After the gypsum and lime were added, the HVFAC was mixed at high speed for 10 min.

TABLE 3 – Mixture proportions of concrete.

Mix	Water (kg/m^3)	Cement (kg/m^3)	Fly Ash (kg/m^3)	Fine Aggregate (kg/m^3)	Coarse Aggregate (kg/m^3)	Gyspum (kg/m^3)	Calcium Hydroxide (kg/m^3)	Glenium 7500 ($liter/m^3$)
CC	201	449	-	655	1033	-	-	-
HVFAC-H	201	136	317	655	1033	14	35	-
HVFAC-L	134	92	213	735	1103	9	23	0.66

FABRICATION AND CURING OF TEST SPECIMENS

The beam splice specimens were constructed and tested in the Structural Engineering High-Bay Research Laboratory (SERL) at Missouri University of Science and Technology. After casting, the specimens and the quality control/quality assurance companion cylinders (ASTM C39 [25] and C78 [26]) and beams (ASTM C496 [27]) were covered with both wet burlap and a plastic sheet. All of the full-scale specimens and companion cylinders and beams were moist cured for 3 days and, after formwork removal, were stored in a semi-controlled environment with a temperature range of 18°C to 24°C and a relative humidity range of 30 % to 50 %, until they were tested at an age of 28 days.

FRESH AND HARDENED PROPERTIES

Table 4 presents the fresh and hardened strength properties of the CC and HVFAC mixes.

TABLE 4 – Fresh and hardened concrete properties.

Property	CC	HVFAC-H	HVFAC-L
Slump (mm)	114	127	139
Air content (%)	1.5	1.5	3.5
Unit weight (kg/m3)	2390	2340	2451
Split cylinder strength[a] (kPa)	2650	2400	2100
Flexural strength[b] (kPa)	2850	2450	2950
Compressive Strength[a] (MPa)	30.9	23.9	23.6

[a]Values represent the average of three cylinders (ASTM C39 [32] and C496 [34]).
[b]Values represent the average of three beams (ASTM C78 [33]

TEST SETUP AND PROCEDURE

A load frame was assembled and equipped with two 490-kN, servo-hydraulic actuators intended to apply the two-point loads to the beams. The load was applied in a displacement control method at a rate of 0.50mm/min. The beams were supported on a roller and a pin support, 300mm from each end of the beam, creating a four-point loading situation with the two actuators. An LVDT was used to measure the deflection at the beam center and strain gages were installed at both ends of each splice to monitor the strain in the longitudinal reinforcement during the test. Figure 1 shows both the beam loading pattern and the location of the strain gages. During the test, any cracks that formed on the surface of the beam were marked at load increments of approximately 22 kN, and both the deformation and strains were monitored until the beam reached failure.

TEST RESULTS AND DISCUSSIONS

All of the beams failed in bond, experiencing a splitting failure. Based upon data collected from the strain gages, none of the longitudinal reinforcement reached yield at failure. Figure 2(b) shows the load–deflection behavior for the beams (the deflection was measured at midspan) for both the HVFAC and the CC specimens. Before the first flexural cracks occurred (point A), all of the beams displayed a steep linear elastic behavior. After the appearance of flexural cracks in the maximum moment region, by increasing the load, new flexural cracks were formed between the two point loads. Upon further increasing the applied load, a bond failure occurred. As Fig. 2(b) reveals, the load–deflection behavior of the HVFAC and CC beams was essentially identical except for the value at failure. Similarly, the cracking patterns experienced by the HVFAC and CC were essentially identical, as shown in Fig. 3. All of the beams displayed a horizontal splitting failure along the length of the longitudinal splice.

Table 6 summarizes the longitudinal reinforcement stress at bond failure as determined from the strain gages, where the specimen designation “Top” refers to the specimen cast upside down to evaluate the top bar effect. Also included in Table 6 are calculated steel stresses based on a moment–curvature approach, with the first calculated value based on the Popovic, Thorenfeldt, and Collins stress–strain curve, and the second

calculated value based on the Hognested stress– strain curve (ACI 408R [21] recommended method). Furthermore, to compare the bond strength of the HVFAC and CC specimens, the test results were normalized with both the square root and fourth root of the compressive strength of the concrete.

Test results show that the high cementitious content HVFAC beams had 29 % and 48 % higher average longitudinal reinforcement stress compared with the CC beams when normalized by the square root of the compressive strength of the concrete for bottom and top reinforcement bars, respectively. When normalized with the fourth root of the concrete compressive strength, the high cementitious content HVFAC beams had 21 % and 39 % higher average longitudinal reinforcement stress compared with the CC beams for bottom and top reinforcement bars, respectively.

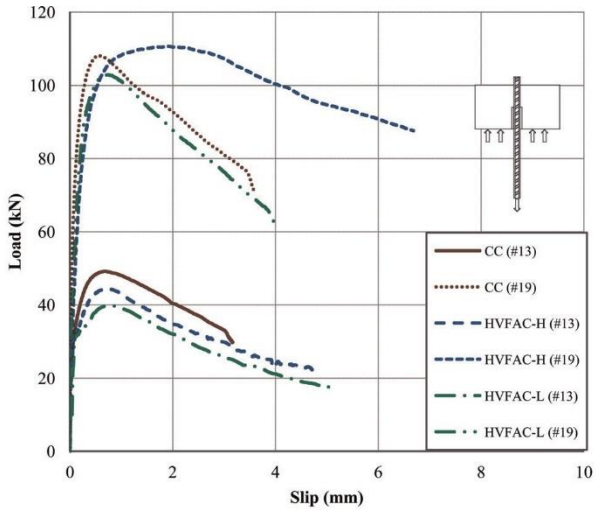

a) Pull-out Test

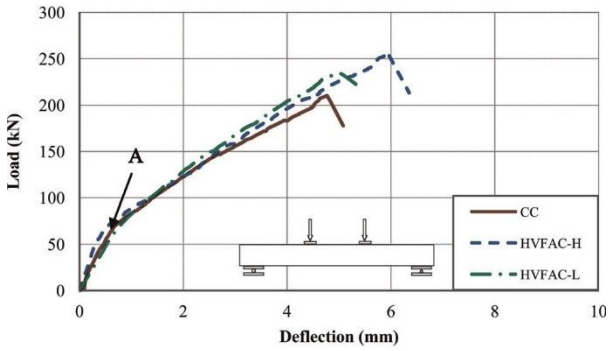

b) Splice Specimen Test

FIG. 2 – Load deflection of the specimens.

For the low cementitious content HVFAC beams, the average longitudinal reinforcement stress increased 15 % and 23 % compared with the CC beams when normalized by the square root of the compressive strength of the concrete for bottom and top reinforcement bars, respectively. When normalized with the fourth root of the concrete

compressive strength, the low cementitious content HVFAC beams had 8 % and 15 % higher longitudinal reinforcement stress compared with the CC beams for bottom and top reinforcement bars, respectively.

a) CC **b) HVFAC-H** **b) HVFAC-L**

FIG. 3 – Crack pattern of the beams at bond failure.

TABLE 5 – Longitudinal reinforcement stress (MPa)

		Measured[a]		Calculated (Moment-Curvature Method)				Measured[a]	
Section		Measured[a]	Average	(M-Φ)[b]	Average	(M-Φ)[c]	Average	$\frac{f_s}{\left(f'_c/f'_{c(design)}\right)^{1/2}}$	$\frac{f_s}{\left(f'_c/f'_{c(design)}\right)^{1/4}}$
CC	1	376	356	304	292	375	363	337	346
	2	335		279		350			
	Top	332	332	278	278	348	348	314	323
HVFAC-H	1	430	405	333	334	397	398	436	420
	2	380		335		399			
	Top	433	433	360	360	422	422	466	449
HVFAC-L	1	372	358	328	314	390	376	387	372
	2	344		300		362			
	Top	356	356	326	326	388	388	385	370

[a]Strain (from strain gauges) multiplied by the modulus of elasticity.
[b]Popovic, Thorenfeldt, and Collins stress-strain curve.
[c]Hognested stress-strain curve (ACI 408R [21] recommended method).

For the low cementitious content HVFAC beams, the average longitudinal reinforcement stress increased 15 % and 23 % compared with the CC beams when normalized by the square root of the compressive strength of the concrete for bottom and top reinforcement bars, respectively. When normalized with the fourth root of the concrete compressive strength, the low cementitious content HVFAC beams had 8 % and 15 % higher longitudinal reinforcement stress compared with the CC beams for bottom and top reinforcement bars, respectively.

The top bar effect did not occur for the HVFAC specimens in this study. In fact, for all the HVFAC specimens, the top bars had either identical or even slightly higher bond strength than the bottom bars. In general, the top bar effect is caused by the accumulation of bleed water trapped beneath the underside of the reinforcing steel [21]. The trapped water reduces bond along this interfacial transition zone and, even more importantly, reduces the local strength of the concrete, in particular the tensile strength. Tensile strength of the concrete plays a critical role in bond splitting failures [21]. Fly ash, particularly large amounts of fly ash, increases the tortuosity of the capillary system within the concrete, rendering the system disconnected and decreasing the resulting capillary porosity [28 – 30]. This change in the capillary system results in a significant

decrease in water migration during hydration, particularly for concretes with water–cementitious-material ratios of 0.40 or less [29,30], thus significantly reducing the top bar effect. However, because of the limited number of top bar specimens used in this study—one for each concrete type—further research is needed to reach a definitive conclusion.

Table 6 presents the ratio of experimental-to-theoretical stress in the longitudinal reinforcement, with the theoretical value based on the moment–curvature analysis. The table includes analysis results based on two different stress–strain diagrams. The authors investigated both models to determine whether any noticeable differences resulted based on the assumed stress–strain diagram. The measured stresses are based on the strain gages installed at the start of each splice (see Fig. 2). Even with the potential for slight inaccuracies in the strain gage readings caused by localized cracking and the slight reduction in cross section required for mounting the gages, the measured readings offer a valuable basis of comparison with the moment–curvature results. Based on the strain gage measurements, results from the Popovic, Thorenfeldt, and Collins stress–strain curve underestimated the longitudinal reinforcement stress by approximately 20 %, but the bar stress calculated based on the Hognested stress–strain curve had excellent agreement with the longitudinal reinforcement stress calculated based on the strain gages, with experimental-to-theoretical stress ratios ranging from 0.92 to 1.02.

TABLE 6 – Experimental-to-theoretical ratio of longitudinal reinforcement stress.

Section		$\left(\frac{f_{s(test)}}{f_{s(M-\varphi)}}\right)_{avg}$ [a]	$\left(\frac{f_{s(test)}}{f_{s(M-\varphi)}}\right)_{avg}$ [b]
CC	1	1.22	0.98
	2		
	Top	1.19	0.95
HVFAC-H	1	1.21	1.02
	2		
	Top	1.20	1.02
HVFAC-L	1	1.14	0.95
	2		
	Top	1.09	0.92
Average		1.18	0.97
COV (%)		4.2	4.3

[a]Popovic, Thorenfeldt, and Collins stress–strain curve.
[b]Hognested stress–strain curve (ACI 408R [21] recommended method).

COMPARISON OF TEST RESULTS WITH BOND TEST DATABASE

Figure 5 presents the longitudinal steel reinforcement stress versus compressive strength of concrete for this study, as well as the wealth of bond test data available in the literature [21]. Given the significant scatter of the database of previous bond test results, it is somewhat difficult to draw definitive conclusions on the current test values.

Nonetheless, visually, Fig. 5 seems to indicate that the CC and HVFAC test results follow the same general trend of increasing bond strength as a function of the compressive strength of the concrete. Furthermore, statistical analysis of the data indicates that only one of the CC test results fall below a 95 % confidence interval of a nonlinear regression curve fit of the database. The low cementitious content HVFAC and the other two CC test results fall within a 95 % confidence interval of the nonlinear regression curve fit. However, all of the high cementitious content test results fall above a 95 % confidence interval of the nonlinear regression curve fit of the database. As a result, it would appear that the bond strength of HVFAC for the beams tested in this study is comparable or greater than CC.

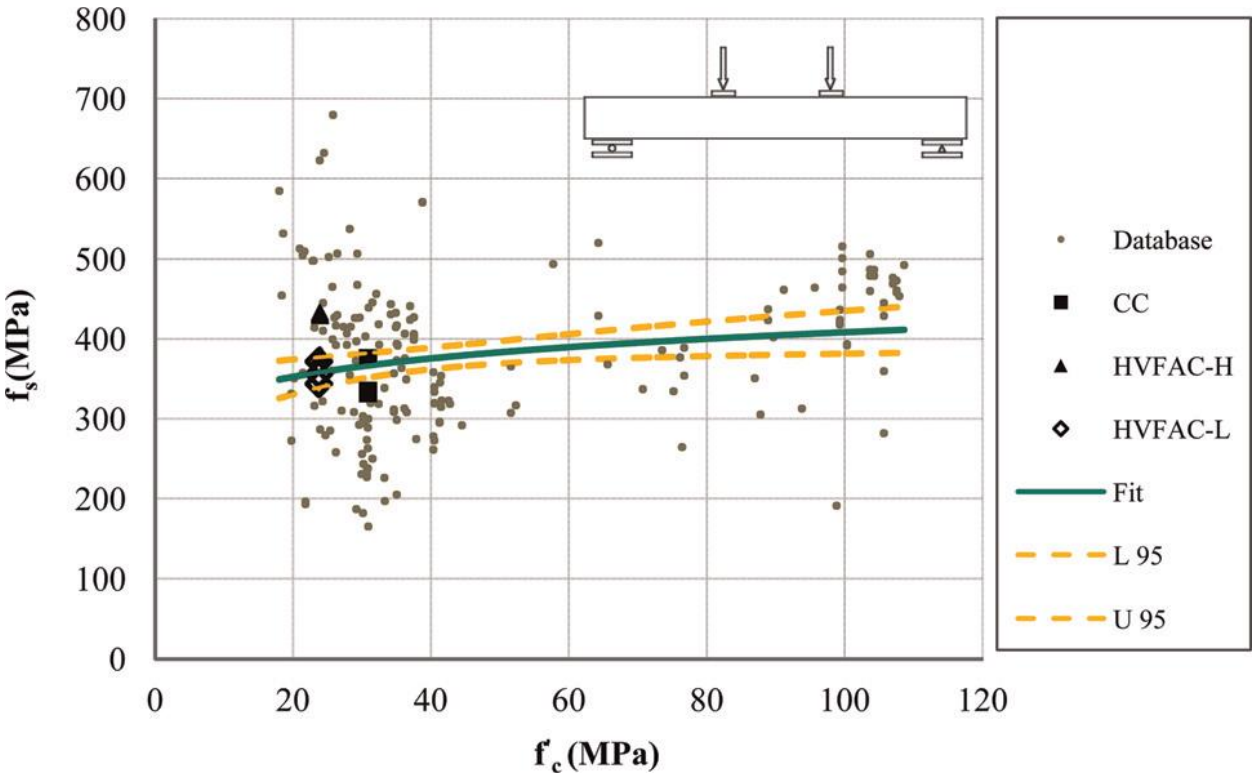

FIG. 4 – Longitudinal steel-reinforcement stress versus compressive strength of concrete (database of ACI 408 and test results of this study).

FIINDINGS AND CONCLUSIONS

To study the bond strength of reinforcing steel in HVFAC, nine full-scale beams (both CC and HVFAC) were constructed and tested to failure. Based on the results of this study, the following findings and conclusions are presented:

- The HVFAC (both high and low cementitious content) beams had higher average longitudinal reinforcement steel stress compared with the CC beams.
- The high cementitious content HVFAC beams had greater average longitudinal reinforcement steel stress than the low cementitious content HVFAC beams.

- The top bar effect did not occur for the HVFAC specimens in this study, primarily as a result of the decreased capillary porosity of the mixes containing the high volumes of fly ash.
- The load–deflection behavior of the HVFAC and CC beams was essentially identical except for the value at failure. Similarly, the cracking patterns experienced by the HVFAC and CC beams were essentially identical, with all of the specimens displaying a horizontal splitting failure along the length of the longitudinal splice.
- The measured longitudinal reinforcement stress at bond failure had excellent agreement with the moment–curvature method based on the Hognested stress–strain curve.
- Based on the strain gage measurements, the moment–curvature method based on the Popovic, Thorenfeldt, and Collins stress–strain curve underestimated the longitudinal reinforcement stress by approximately 20 % compared with the measured bar stress at bond failure.

For the specimens studied in this investigation, the HVFAC showed improved bond performance over the CC. However, because of the limited nature of the data set regarding aspect ratio, mix designs, aggregate type and content, etc., investigated, the researchers recommend further testing to increase the database of test results.

ACKNOWLEDGMENTS

The writers gratefully acknowledge the financial support provided by the Missouri Department of Transportation (MoDOT) and the National University Transportation Center at Missouri University of Science and Technology. The writers also thank the support staff in the Department of Civil, Architectural and Environmental Engineering and Center for Infrastructure Engineering Studies at Missouri S&T for their efforts. The conclusions and opinions expressed in this paper are those of the writers and do not necessarily reflect the official views or policies of the funding institutions.

REFERENCES

[1] USGS, “Minerals Yearbook, Cement,” U.S. Geological Survey, United States Department of the Interior, Washington, D.C., 2012, pp. 38–39.

[2] Marland, G., Boden, T. A., and Andres, R. J., 2008, “Global, Regional, and National Fossil Fuel CO2 Emissions. In Trends: A Compendium of Data on Global Change,” Carbon Dioxide Information Analysis Center, Oak Ridge National Laboratory, United States Department of Energy, Oak Ridge, TN, http://cdiac.ornl.gov/trends/emis/overview.html (Last accessed March 2012).

[3] Hanle, L., Jayaraman, K., and Smith, J., 2012, “CO2 Emissions Profile of the U.S. Cement Industry,” http://infohouse.p2ric.org/ref/43/42552.pdf (Last accessed March 2012).

[4] Bilodeau, A. and Malhotra, V. M., “High-Volume Fly Ash System: Concrete Solution for Sustainable Development,” ACI Mater. J., Vol. 97, 2000, pp. 41–48.

[5] ASTM 618-94a, 1995, “Standard Specification for Coal Fly Ash and Raw or Calcined Natural Pozzolan for Use as a Mineral Admixture in Portland Cement Concrete,” Annual Book of ASTM Standards, Vol. 04.02, ASTM International, West Conshohocken, PA, pp. 304–306.

[6] ACI 232.2R, 2003, “Use of Fly Ash in Concrete,” American Concrete Institute, Farmington Hills, MI.

[7] Dunstan, E., “Fly Ash and Fly Ash Concrete,” Report No. REC-ERC-82-1, Bureau of Reclamation, Denver, CO, 1984, 42 pp.

[8] Dunstan, E. R., Jr., “Performance of Lignite and Sub-Bituminous Fly Ash in Concrete,” Report No. REC-ERC-76, U.S. Bureau of Reclamation, Denver, CO, 1976, 23 pp.

[9] Dunstan, E. R., Jr., “A Possible Method for Identifying Fly Ashes that Will Improve the Sulfate Resistance of Concretes,” Cement, Concrete, Aggregates, Vol. 2, No. 1, 1980, pp. 20–30.

[10] Dunstan, M. R. H., “Rolled Concrete for Dams—A Laboratory Study of High Fly Ash Concrete,” Technical Note No. 105, Construction Industry Research and Information Association, London, 1981, 96 pp.

[11] Dunstan, M. R. H., “Rolled Concrete for Dams—Construction Trials Using High Fly Ash Content Concrete,” Technical Note No. 106, Construction Industry Research and Information Association, London, 1981, 94 pp.

[12] Berry, E. E., Hemmings, R. T., Zhang, M. H., Cornelious, B. J., and Golden, D. M., “Hydration in High-Volume Fly Ash Binders,” ACI Mater. J., Vol. 91, 1994, pp. 382–389.

[13] ACI 211.4R-08, Guide for Selecting Proportions for High-Strength Concrete With Portland Cement and Fly Ash, American Concrete Institute, Farmington Hills, MI, 2008.

[14] Myers, J. J. and Carrasquillo, R. L., “Mix Proportioning for High-Strength HPC Bridge Beams,” American Concrete Institute Special Publication 189, American Concrete Institute, Detroit, MI, 1999, pp. 37–56.

[15] Malhotra, V. M., “Superplasticized Fly Ash Concrete for Structural Applications,” Concrete Int., Vol. 8, 1986, pp. 28–31.

[16] Li, S., Roy, D. M., and Kumer, A., “Quantitative Determination of Pozzolanas in Hydrated System of Cement or Ca(OH)2 with Fly Ash or Silica Fume,” Cement Concrete Res., Vol. 15, 1985, pp. 1079–1086.
[17] Gopalan, M. K., “Nucleation and Pozzolanic Factors in Strength Development of Class F Fly Ash Concrete,” ACI Mater. J., Vol. 90, 1993, pp. 117–121. LOONEY ET AL. ON AN EXPERIMENTAL STUDY 15
[18] Naik, T. R., Singh, S. S., and Sivasundaram, V., “Concrete Compressive Strength, Shrinkage and Bond Strength as Affected by Addition of Fly Ash and Temperature,” The University of Wisconsin–Milwaukee, Milwaukee, WI, 1989.
[19] Cross, D., Stephens, J., and Vollmer, J., “Structural Applications of 100 Percent Fly Ash Concrete,” Montana State University, Bozeman, MT, 2005.
[20] Gopalakrishnan, S., “Demonstration of Utilising High Volume Fly Ash Based Concrete for Structural Applications,” Structural Engineering Research Centre, Chennai, India, 2005.
[21] ACI 408R, “Bond and Development of Straight Reinforcing Bars in Tension,” American Concrete Institute, Farmington Hills, MI, 2003.
[22] ACI 318/318R, “Building Code Requirements for Structural Concrete ACI 318-08 and Commentary 318R-08,” American Concrete Institute ACI Committee, American Concrete Institute, Farmington Hills, MI, 2008, pp. 155–168.
[23] ASTM A615/A615M, 2009, “Standard Specification for Deformed and Plain Carbon-Steel Bars for Concrete Reinforcement,” Annual Book of ASTM Standards, Vol. 01.04, ASTM International, West Conshohocken, PA, 6 pp.
[24] Bentz, D. P., “Powder Additions to Mitigate Retardation in High-Volume Fly Ash Mixtures,” ACI Mater. J., Vol. 107, No. 5, 2010, pp. 508–514.
[25] ASTM C39/C39M, 2012, “Standard Test Method for Compressive Strength of Cylindrical Concrete Specimens,” Annual Book of ASTM Standards, Vol. 04.02, ASTM International, West Conshohocken, PA, 7 pp.
[26] ASTM C78/C78M, 2010, “Standard Test Method for Flexural Strength of Concrete (Using Simple Beam with Third-Point Loading,” Annual Book of ASTM Standards, Vol. 04.02, ASTM International, West Conshohocken, PA, 4 pp.
[27] ASTM C496/C496M, 2011, “Standard Test Method for Splitting Tensile Strength of Cylindrical Concrete,” Annual Book of ASTM Standards, Vol. 04.02, ASTM International, West Conshohocken, PA, 5 pp.
[28] Malhotra, V. M. and Mehta, P. K., High-Performance, High-Volume Fly Ash Concrete for Building Sustainable and Durable Structures, 3rd Ed., Supplementary Cementing Materials for Sustainable Development, Inc., Ottawa, Canada, 2008.
[29] Bentz, D. P. and Weiss, J., “Internal Curing: A 2010 State of the Art Review,” NISTIR 7765, National Institute of Standards and Technology, U.S. Department of Commerce, Gaithersburg, MD, 2011.
[30] De la Varga, I., Castro, J., Bentz, D., and Weiss, J., “Application of Internal Curing for Mixtures Containing High Volumes of Fly Ash,” Cement Concrete Compos., Vol. 34, 2012, pp. 1001–1008.